NATURE OF EARTHQUAKES AND SEISMIC HAZARDS 2

by Bruce A. Bolt and Douglas Dreger

2.1 INTRODUCTION

Seismology has long contributed to engineering and architecture. The founders of seismology, defined as the scientific study of earthquakes, were Robert Mallet [1810-1881], a civil engineer, and John Milne [1850-1913], a mining engineer. They were first stimulated by their field studies of great earthquakes, and then posed some basic questions, such as "What is the mechanical explanation for the damage (or lack of it) when structures are subject to seismic strong ground motion?" and "What are the essential characteristics of seismic waves that affect different structures?"

Robert Mallet, after the great Neapolitan earthquake of 1857 in southern Italy, endeavored to explain "the masses of dislocated stone and mortar" that he observed in terms of mechanical principles and the building type and design. In doing so, he established much basic vocabulary, such as **seismology**, **hypocenter** (often called the earthquake **focus**), and **isoseismal** (contours of equal seismic intensity). These nineteenth century links between seismology, engineering, and architecture have continued ever since.

A later well-known architectural example is Frank Lloyd Wright's design of the Imperial Hotel in Tokyo (Figure 2-1).
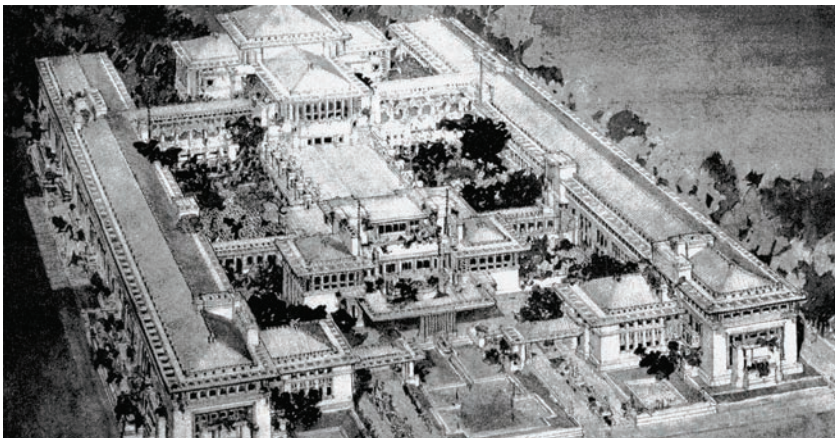

Figure 2-1

Imperial Hotel, Tokyo

SOURCE: FRANK LLOYD WRIGHT FOUNDATION

During the planning of his ornate edifice, Wright felt many earthquakes and noted that "the terror of temblors never left me as I was planning the building." He knew that the site of the hotel would be exceptionally dangerous in an earthquake because eight feet of topsoil overlaying 60 feet of soft mud would not offer firm support. To meet this threat, he introduced a number of innovations, including shallow foundations on broad footings, supported by small groups of concrete pilings along the foundation wall. Rather than unreinforced brick walls, the building had double-course walls composed of two outer layers of brick bonded in the middle, with a core of reinforcing bars set in concrete. He designed the first floor walls to be rigid and thick; the walls of higher floors tapered upwards and contained fewer windows. He topped the structure with a hand-worked green copper roof.

Wright was also among the first architects to appreciate that the mechanical systems in buildings, such as plumbing and wiring, could be hazards in earthquakes. To lessen this risk, he ran the hotel pipes and wires through trenches or hung them from the structure so that "any disturbance might flex and rattle but not break the pipes and wiring." He also conceived the beautiful reflecting pool at the front of hotel as a reservoir of water for fire fighting.

Less than nine months after the opening of the Imperial Hotel, the Great 1923 Kanto earthquake caused enormous devastation in the Tokyo area, shattering over 5,000 buildings and creating a firestorm. The merit of Wright's reflecting pool became clear. The Imperial Hotel still stood after its battering in the earthquake, although the damage and cracking within the building was considerable.

Nowadays, seismologists can offer the architect and engineer more reliable quantitative knowledge than in 1923 concerning the earthquake hazard at a particular site, and also the patterns and intensities of the earthquake waves that are likely to shake the structure. To a large extent this is due to recent availability of more instrumental recordings of intense seismic wave motions in various geological conditions, especially near to their fault sources.

The aim of this chapter is to provide some of the latest knowledge about earthquakes that may be most relevant to architectural design. The intent is that the description should serve architects when they discuss

with their clients the appropriateness of certain designs, in relation to a seismic hazard. Toward this goal the discussion covers faulting (the main cause of earthquakes) an explanation of the types of waves generated by the fault rupture, the effect of soils on the strong ground motions, and contemporary methods of estimating earthquake risk.

References are also provided to a number of research papers and books for the architect who wants to pursue the subject more deeply. Several relevant addresses of web pages on earthquakes, of which there is a diverse and growing number, are also included.

2.2 OBSERVATIONS OF EARTHQUAKES

2.2.1 Plate Tectonics and Seismicity

A coherent global explanation of the occurrence of the majority of earthquakes is provided by the geological model known as Plate Tectonics. The basic concept is that the Earth's outermost part (called the lithosphere) consists of several large and fairly stable rock slabs called plates. The ten largest plates are mapped in Figure 2-2. Each plate extends to a depth of about 100-200 km and includes the Earth's outermost rigid rocky layer, called the crust.

The moving tectonic plates of the Earth's surface also provide an explanation of the various mechanisms of most significant earthquakes. Straining and fracturing of the regional crustal rocks result from collisions between adjacent lithospheric plates, from destruction of rocky slab-like plate as it descends or **subducts** into a dipping zone beneath island arcs, and from spreading out of the crust along mid-oceanic ridges. In the United States, the most significant subduction zone is the Cascadia Zone in western Washington state, where the Juan de Fuca Plate slides (or subducts) under the America Plate (Figure 2-2). Research indicates that ruptures along this zone have resulted in very large magnitude earthquakes about every 500-600 years . The 1964 Alaska earthquake was in a subduction zone and was responsible for the greatest recorded United States earthquake. The earthquakes in these tectonically active boundary regions are called **interplate earthquakes**. The very hazardous shallow earthquakes of Chile, Peru, the eastern Caribbean, Central America, Southern Mexico, California, Southern Alaska, the Aleutians the Kuriles, Japan, Taiwan, the Philippines, Indonesia, New
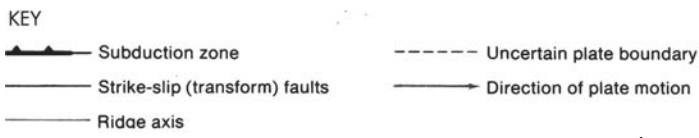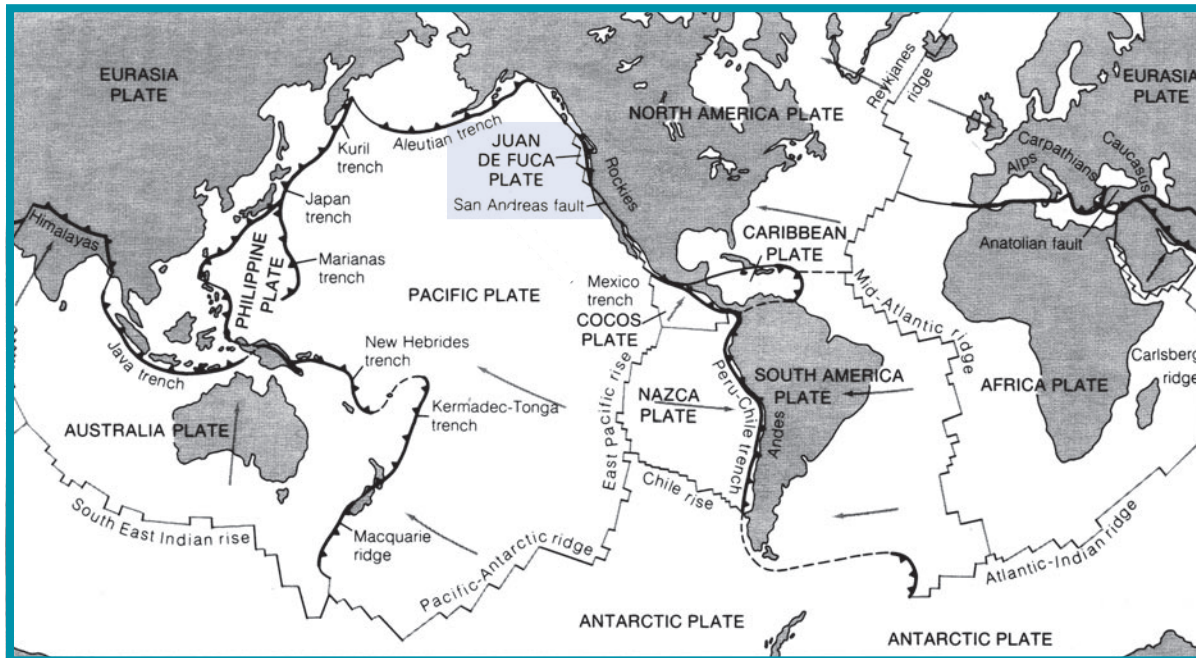
Figure 2-2: The major tectonic plates, midoceanic ridges, trenches and transform faults.

Zealand, the Alpine-Caucasian-Himalayan belt are of plate-edge type. Earthquakes generated at depths down to 700 km also occur along plate edges by a mechanism yet unclear.

As the mechanics of the lithospheric plates have become better understood, long-term predictions of the place and size of interplate earthquakes become possible. For example, many plates spread toward the subduction zones at long-term geologic rates of from 2 to 5 cm (about one to two inches) per year. Therefore, in active arcs like the Aleutian and Japanese islands and subduction zones like Chile and western Mexico, the history of large earthquake occurrence can identify areas that currently lag in earthquake activity.

NATURE OF EARTHQUAKES AND SEISMIC HAZARDS

There is a type of large earthquake that is produced by slip along faults connecting the ends of offsets in the spreading oceanic ridges and the ends of island arcs or arc-ridge chains (see Figure 2-2). In these regions, plates slide past each other along what are called **strike–slip**, or **transform faults**. Considerable work has been done on the estimation of strong ground motion parameters for the design of critical structures in earthquake-prone countries with either transform faults or ocean-plate subduction tectonics, such as Japan, Alaska, Chile, Mexico, and the United States. Similar hazard studies have been published for the Himalaya, the Zagros (Iran), and Alpine regions all examples of mountain ranges formed by **continent-to-continent collisions**. Such collision zones are regions where very damaging earthquakes sometimes occur.

While simple plate-tectonic theory provides a general understanding of earthquakes and volcanoes, it does not explain all seismicity in detail, for within continental regions, away from boundaries, there are also large devastating earthquakes. These **intraplate** earthquakes can be found on nearly every continent (Yeats et al., 1997). The disastrous Bhuj (M = 7.7) earthquake in northeast India in the seismically active Kutch province was a recent example of such an intraplate earthquake (see Section 2.3.3 for an explanation of earthquake magnitude (M). In the United States, the most famous intraplate earthquakes occurred in 1811-1812 in the New Madrid area of Missouri, along the Mississippi River; another is the-damaging 1886 Charleston, South Carolina, earthquake. The Nisqually earthquake of 2001 that took place in Washington was a deep focus earthquake with a moment magnitude of 6.8. However, because of its depth of focus (32 miles), structural damage to buildings was not widespread and modern buildings and those recently upgraded performed well.

Shallow-focus earthquakes (focus depth less than 70 km) wreak the most devastation, and they contribute about three-quarters of the total energy released in earthquakes throughout the world. In California, for example, all of the known damaging earthquakes to date have been shallow-focus. In fact, it has been shown that the great majority of earthquakes occurring in California originate from foci in the upper ten kilometers of the Earth's crust, and only a few are as deep as 15-20 km, excepting those associated with subduction north of Cape Mendocino.

All types of tectonic earthquakes defined above are caused by the sudden release of elastic energy when a fault ruptures; i.e. opposite sides rapidly

slip in opposite directions. This slip does work in the form of heat and wave radiation and allows the rock to rebound to a position of less strain.

Most moderate to large shallow earthquakes are followed, in the ensuing hours and even in the next several months, by numerous, usually smaller, earthquakes in the same vicinity. These earthquakes are called **aftershocks**, and large earthquakes are sometimes followed by very large numbers of them. The great Rat Island earthquake caused by subduction under the Aleutian Islands on 4 February 1965 was, within the next 24 days, followed by more than 750 aftershocks large enough to be recorded by distant seismographs. Aftershocks are sometimes energetic enough to cause additional damage to already weakened structures. This happened, for example, a week after the Northridge earthquake of 17 January 1994 in the San Fernando Valley, when some weakened structures sustained additional cracking from magnitude 5.5-6.0 aftershocks. A few earthquakes are preceded by smaller **foreshocks** from the source area, and it has been suggested that these can be used to predict the main shock, but attempts along this line have not proven statistically successful.

Volcanoes and earthquakes often occur together along the margins of plates around the world that are shown in Figure 2-2. Like earthquakes, there are also intraplate volcanic regions, such as the Hawaiian volcanoes in which earthquakes and volcanic activity are clearly physically related.

2.2.2 Earthquake Fault Types

The mechanical aspects of geological faults are the key factors in understanding the generation of strong seismic motions and modeling their different characteristics. Some knowledge of the fault type to be encountered at a site is useful to the architect because of the different types and intensities of motion that each fault type may generate.

First, the geometry of fault-slip is important (see Figure 2-3). The **dip** of a fault is the angle that the fault surface makes with a horizontal plane, and the **strike** is the direction of the fault line exposed or projected at the ground surface relative to the north. A **strike-slip** or **transform** fault involves displacements of rock laterally, parallel to the strike. If, when we stand on one side of a fault and see that the motion on the other side is from left to right, the fault is **right-lateral** strike-slip. If the motion on the other side of the fault is from right to left, the fault is termed a left-lateral strike slip. Events of strike-slip type include the 1857 and 1906 San
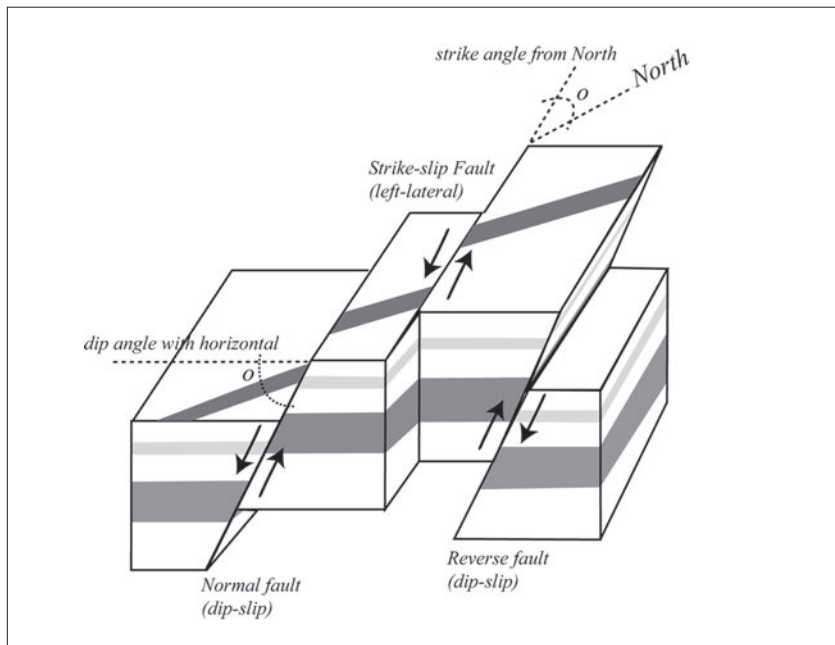
Figure 2-3: The three primary fault types.

The strike is the angle the surface trace of the fault makes with respect to geographic north. The dip is the angle the fault plane makes in the vertical with respect to the horizintal.

SOURCE: Bruce A. Bolt, *Earthquakes*, 2003

Andreas fault, California, earthquakes and more recently the 1996 Kobe, Japan ($M_W = 6.9$), 1999 Izmit, Turkey ($M_W = 7.6$, Figure 2-4), and 2002 Denali, Alaska ($M_W = 7.9$), earthquakes.

The **right-lateral** displacement of the North Anatolian fault in Turkey from the 1999 event is shown in Figure 2-4. Catastrophic damage to multi-story buildings both near and across the fault resulted from the fault motions. A lone standing building in the foreground demonstrates that variation in building construction is also a factor in the survivability of a structure.

A **dip-slip** fault is one in which the motion is largely parallel to the dip of the fault and thus has vertical components of displacement. There are two types of dip-slip faults: the normal and the **reverse** fault.

Figure 2-4: Izmit, Turkey, 1999.

The right-lateral strike-slip fault motion (depicted by white arrows and evidenced by the offset masonry wall) pass through a collapsed structure. Note that collapsed and standing structures adjacent to the fault demonstrate both the severity of ground shaking and variation in the quality of construction.

A normal fault is one of dip-slip type in which the rock above the inclined fault surface moves downward relative to the underlying crust. Faults with almost vertical slip are also included in this category. The Borah Peak (M_W = 7.3) earthquake in Idaho in 1983 is an example of a normal-type event that produced a scarp six feet high.

In a reverse fault, the crust above the inclined fault surface moves upward relative to the block below the fault. **Thrust** faults belong to this category but are generally restricted to cases when the dip angle is small. In **blind thrust faults**, the slip surface does not penetrate to the ground surface (for example, in the 1994 Northridge earthquake).

For the common shallow crustal earthquakes, seismic ground motions differ systematically when generated by strike-slip, thrust, or normal mechanisms. Given the same earthquake magnitude, distance to the site, and site condition, the ground motions from thrust earthquakes tend to be (about 20-30 percent) larger than the ground motions from strike-slip earthquakes, and the ground motions from normal faulting earthquakes tend to be smaller (about 20 percent) than the ground motions from strike-slip earthquakes. For subduction earthquakes such as the 1964 Alaska (M_W = 9.2) event, the ground motions systematically differ from those generated by interface or intra-plate earthquakes. Again, for the same magnitude, distance, and site condition, the ground motions from intra-plate earthquakes tend to be about 40 percent larger than the ground motions from inter-plate earthquakes.

NATURE OF EARTHQUAKES AND SEISMIC HAZARDS

Reverse-fault slips have the greatest range of size, because they can grow both in the strike and dip directions. In subduction zones, the largest reverse events occur in the depth range from 0-100 km, with lengths on the order of 1,000 km. The 1960 Chile and 1964 Alaska mega-earthquakes (M_W = 9.5 and M_W = 9.2, respectively) are examples of this type. The 1994 Northridge, California, earthquake, despite its moderate size (M_W = 6.7), inflicted considerable damage and casualties because of its location on a blind thrust beneath a heavily populated region. In most cases however, fault slip is a mixture of strike-slip and dip-slip and is called **oblique** faulting, such as occurred in the 1989 Loma Prieta (M_W = 6.9) earthquake in central California. In the latter case also, the fault slip was not visible at the surface of the ground but was inferred from seismological recordings. Large scale thrusting of the ground surface was very evident along the Chelungpu fault in the 1999 Chi Chi earthquake (M_W = 7.6) in Taiwan (see Figure 2-5).

It is at once obvious that any description of seismicity requires a measure of earthquake size, for comparison between earthquakes and between seismic hazard zones. As in classical mechanics, a suitable quantity to characterize the mechanical work done by the fault rupture that generates the seismic waves is the mechanical moment. In these terms we can

Figure 2-5: This building near Juahan, in Taiwan, was lifted several feet by the fault. Fault rupture runs just near the side of the building, down the alley. The white lines highlight the offset ground surface. There was no apparent damage to the building.

consider the seismic moment that is, as might be expected, proportional to the area of fault slip A multiplied by the slip distance D.

Fault offset a poses high risk for certain types of structures. When such structures, including dams and embankments, must be built across active faults, the design usually incorporates joints or flexible sections in the fault zone. The maximum horizontal offset in the 1906 San Francisco earthquake was about 18 feet.

2.2.3 Earthquake Effects

There are many earthquake effects related to the geology and form of the earth that are of significance for architects. In the most intensely damaged regions, the effects of severe earthquakes are usually complicated. The most drastic effects occur chiefly near he causative fault, where there is often appreciable ground displacement as well as strong ground shaking (e.g. Figure 2-4); at greater distance, noticeable earthquake effects often depend on the topography and nature of the soils, and are often more severe in soft alluvium and unconsolidated sediment basins. Some remarkable effects are produced in bodies of water such as lakes, reservoirs, and the sea.

● Ground Shaking Intensity

Efforts to measure the size of an earthquake by rating microseismic data in the affected area go back to the 19th century. Before the invention of instrumentally based seismic magnitude, the most common historical scale rated the relative "intensity" of an earthquake. This measure is not capable of strict quantitative definition because seismic intensity at a particular point of the Earth's surface depends on many factors, including the source moment M0, area of the rupture fault, the fault mechanism, the frequency-spectrum of wave energy released, the geological conditions, and the soils at a given site.

The most widely used scale historically was originated by Rossi and Forell in 1878. A later modification developed by Mercalli in Italy, now termed the **Modified Mercalli Intensity (MMI)** scale, is suitable for conditions in the United States. Bolt (2003) describes the details of the various intensity measures.

The geographical distribution of intensity is summarized by constructing isoseismal curves, or contour lines, which separate areas of equal inten-

sity. The most probable position of the epicenter and the causative fault rupture is inside the area of highest intensity. An example of MMI curves for two moderate events is given in Figure 2-6. Clearly there can be large regional differences in MMI. Such variations in seismic wave attenuation are discussed in Section 2.6.1.

Correlations have been worked out between measured characteristics of the seismic waves and the reported Modified Mercalli intensity. A common one is that between the maximum ("peak") ground accelera- tion, A (centimeters per second squared), and the MM intensity, I. Such correlations are only broadly successful, particularly at the higher intensities. The description of the seismic waves for architectural and en- gineering purposes depends on a mixture of parameters, many of which are dependent on the frequency of the seismic waves. Nevertheless, b - cause in many parts of the world instrumental measurements of ground
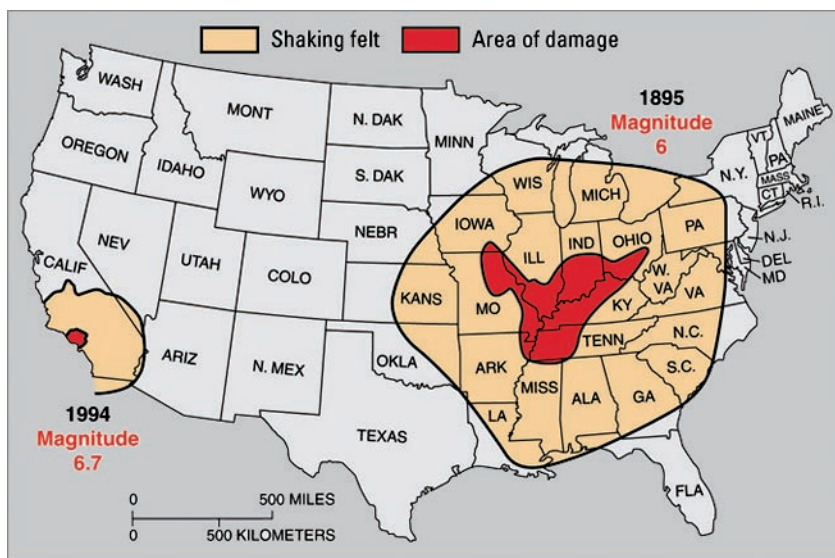

Figure 2-6: Map comparing curves of MMI 3 (shaking felt) and MMI 8 (area of damage) for the magnitude 6.7 1994 Northridge, California, earthquake and a magnitude 6 near New Madrid, Missouri, in 1895. Although the difference in magnitude implies an 11-fold difference in scalar seismic moment, the areas of shaking intensity for the smaller earthquake are substantially larger due to differences in seismic wave attenuation in the non-tectonic region of New Madrid compared to the western U.S. (discussed in section 2.6.1).

SOURCE: USGS FACT SHEET 017-03.

motion are not available, rough seismic intensity remains popular as a descriptor as well as for great historical earthquakes. Peak Ground Acceleration is employed as a measure in the current USGS **Shake-Maps** program, for example: these are maps showing ground shaking intensities that are available on the internet within a few minutes of an earthquake occurrence (see Section 2.6).

A number of other hazards of a geological nature may be triggered by an earthquake occurrence. These may at times cause severe damage and loss of life.

● Landslides

Landslides, ground settlement, and avalanches occur widely with and without earthquakes as a cause. All require special architectural treatment. Landslides and avalanches occur on slopes of a variety of geological materials. For engineering works, the speed at which a landslide develops and moves is a most important feature. Few defenses are available against rapid unexpected movements, but those that move slowly over periods of months to years lend themselves to some precautionary measures. Zoning regulations based on localized geological studies are the most effective mitigation measures.

During an earthquake, a series of seismic waves shakes the ground in all directions, so that under the critical conditions of water saturation, slope, and soil type, even relatively low levels of ground acceleration can cause a landslide. Even if these dynamic accelerations last for only a short time, widespread sliding can occur on marginally stable slopes. During and following the 1971 San Fernando, California, earthquake, for example, thousands of landslides and rockfalls occurred in the San Gabriel Mountains and caused a prominent dust-cloud over the strongly shaken area for days. This was repeated during the nearby 1994 Northridge earthquake.

Another human catastrophe caused by an earthquake-triggered debris avalanche occurred in Peru on May 31, 1970. The earthquake of magnitude 7.7 stimulated a rock avalanche amounting to some 50 million cubic meters of rock, snow, ice, and soil that travelled 15 km from the north peak of Huascarn Mountain, buried the towns around Ranraharca and most of Yungay, and killed at least 18,000 people.

NATURE OF EARTHQUAKES AND SEISMIC HAZARDS

In many instances, smaller landslides and avalanches can be detected in advance by suitable instrumentation installed on the slope with the readings monitored at regular intervals. Means of control can then be applied in appropriate circumstances: for example, removing small volumes of material to relieve the load at the head of the slope and adding material to the toe can be accomplished by earth-moving equipment. For cuts that are man-made, local regulations or ordinances may need to be developed and enforced during construction in a vulnerable area. Slopes made of fill, for example, may be required to be no steeper than 1 vertical to 1-1/2 horizontal, and the fraction of the soil covering the slope must be carefully controlled. Drainage of water away from such slopes is usually specified.

● Tsunamis and Seiches

The occurrence of an earthquake and a sudden offset along a major fault under the ocean floor, or a large submarine landslide, displaces the water like a giant paddle, thus producing powerful water waves at the ocean surface. When they reach a coastline, they may run up on land to many hundreds of meters. The elevation above the tide level (at the time of the tsunami) reached by the water is called the **run-up height**. This vertical distance is not the same as the tsunami water wave height offshore or the horizontal distance of water run-up from the normal water edge.

There have been tsunamis in most oceans of the world, but most notably in the Pacific Ocean. The coastline of Hilo, Hawaii, has seen inundation several times, and the giant earthquake in Alaska in 1964 had a run-up height of six meters in Crescent City, California, killing several people. Near the fault motion, 119 people drowned in Alaska.

A seismic sea wave warning system was set up in the Pacific after the devastating Aleutian tsunami of April 1, 1946. The tsunami warning center in Honolulu provides tsunami alerts and alerts local jurisdictions to issue warnings.

The best disaster prevention measures for a tsunami-prone coast involve zoning that controls the types and sizes of buildings that, if any, are permitted. If a site has a high possibility of tsunami incursion, the designer should consider some of the design provisions against flood, such as elevating the building above an estimated waterline. Of course in the case

of locally generated tsunami, provisions must also be made for the severe strong shaking.

Long-period movements of water can also be produced in lakes and reservoirs by large earthquakes. These oscillations of lake levels are termed **seiches**. The November 2003 Denali earthquake in Alaska generated seismic seiches in wells and lakes of the south central United States. In the 1971 San Fernando, California, earthquake water sloshed out of swimming pools, producing some risk.

● Liquefaction

A notable hazard from moderate to large earthquakes is the liquefaction of water-saturated soil and sand produced by the ground shaking. In an earthquake, the fine-grained soil below the ground surface is subjected to alternations of shear and stress. In cases of low-permeability soils and sand, the water does not drain out during the vibration, building up pore pressure that reduces the strength of the soil.

Because earthquake shaking of significant amplitude can extend over large areas, and fine-grained soils in a saturated state are so widespread in their distribution, liquefaction has frequently been observed in earthquakes. In some cases, it is a major cause of damage and therefore is a factor in the assessment of seismic risk. Liquefaction in the 1964 Alaskan earthquake caused major disruptions of services and utilities and led to substantial building settlements and displacements. In the 1971 San Fernando, California, earthquake, liquefaction of soils in the San Fernando Dam caused a landslide in the upstream portion of the dam structure that almost resulted in a catastrophic dam failure. Widespread liquefaction resulted in severe damage after the 1811-1812 New Madrid and 1886 Charleston, South Carolina, earthquakes.

Many seismic regions have available liquefaction maps so that the risk of liquefaction at building sites can be assessed. Soil engineers have developed various technical methods of controlling liquefaction, the description of which goes beyond this chapter (see Chapter 3).

2.3 SEISMIC WAVES AND STRONG MOTION

2.3.1 Seismic Instrumental Recordings and Systems

Seismographs are instruments that are designed to record ground motions such as accelerations and displacements in earthquakes. Nowadays, technological developments in electronics have given rise to high-precision pendulum seismometers and sensors of both weak and strong ground motion. In these instruments, the electronic voltages produced by motions of a pendulum or the equivalent are passed through electronic circuitry to amplify the ground motion and digitize the signals for more exact measurements.

When seismic waves close to their source are to be recorded, special design criteria are needed. Instrument sensitivity must ensure that the relatively large amplitude waves remain on scale. For most seismological and engineering purposes, the wave frequency is high (1 to 10 Hz, i.e., cycles per second), so the pendulum or its equivalent can be small. For comparison, displacement meters need a pendulum with a long free period (many seconds).

Because many strong-motion instruments need to be placed at unattended sites for periods of months or years before a strong earthquake occurs, they usually record only when a trigger mechanism is actuated with the onset of seismic motion. Solid-state memories are now used with digital recording instruments, making it possible to preserve the first few seconds before the trigger starts the permanent recording. In the past, recordings were usually made on film strips, providing duration of up to a few minutes.

In present-day equipment, digitized signals are stored directly on a memory chip, and are often telemetered to central recording sites in near real-time (several to tens of seconds). In the past, absolute timing was not provided on strong-motion records but only accurate relative time marks; the present trend, however, is to provide Universal (Greenwich Mean) Time - the local mean time of the prime meridian by means of special radio receivers or Global Positioning Satellite (GPS) receivers.

The prediction of strong ground motion and response of engineered structures in earthquakes depends critically on measurements of the lo-

cational variation of earthquake intensities near the fault. In an effort to secure such measurements, special arrays of strong-motion seismographs have been installed in areas of high seismicity around the world, both away from structures **(free field)** and on them (Figure 2-7). The seismic instrumentation of various types of buildings is clearly to be encouraged by architects, both for post-earthquake performance evaluation, future design modification and improved emergency response.

It is helpful for the user of strong-motion **seismograms** (called "**time histories**") to realize that the familiar "wiggly line" graphic records are not the actual motion of the ground, but have been filtered in some way by both the recording instrument and by the agency providing the data (see Section 2.6). In most cases, however, for practical applications the architect or engineer need not be concerned about the difference.
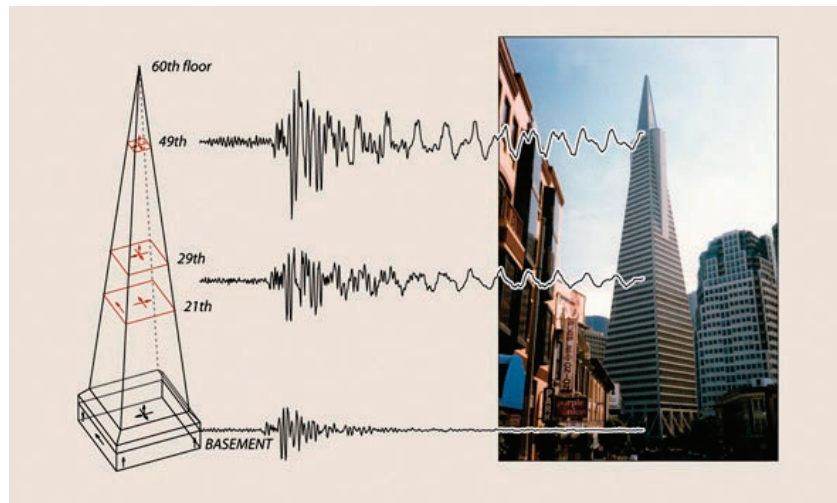

Figure 2-7: Transamerica "Pyramid" building in downtown San Francisco.

 Modern instruments capable of recording large motions strategically placed in structures provide information on the structural response. In this case it is evident that there is amplification of both short-period and long-period motions in the upper floors. Also the duration of shaking at periods corresponding to characteristic vibrations of the structure become quite long towards the top.

SOURCE: USGS FACT SHEET 017-03.

NATURE OF EARTHQUAKES AND SEISMIC HAZARDS

2.3.2 Types of Earthquake Waves

In most instances of seismic ground motions in solid rock or soil, the waves involved are made up of four basic types of elastic waves that create the shaking that people feel and that causes damage in an earthquake. These waves are similar in many important ways to the waves observed in air, water, and elastic solids.

The first two types of waves travel through the body of the earth before arriving at the surface. The faster of these "body" waves is appropriately called the **primary** or P wave (Figure 2-8a). Its motion is the same as that of a sound wave in that, as it spreads out, it alternately pushes (compresses) and pulls (dilates) the rock. These **P** waves, just like acoustic waves, are able to travel through solid rock, such as granite and alluvium, through soils, and through liquids, such as volcanic magma or the water of lakes and oceans.

The second and slower seismic body wave through the earth is called the **secondary** or **S** wave or sometimes the **shear wave** (Figure 2-8b). As an S wave propagates, it shears the rocks sideways at right angles to the direction of travel. At the ground surface, the upward emerging S waves also produce both vertical and horizontal motions. Because they depend on elastic shear resistance, S waves cannot propagate in liquid parts of the earth, such as lakes. As expected from this property, their size is significantly weakened in partially liquefied soil. The speed of both P and S seismic waves depends on the density and elastic properties of the rocks and soil through which they pass. In earthquakes, P waves move faster than S waves and are felt first. The effect is similar to a sonic boom that bumps and rattles windows. Some seconds later, S waves arrive with their significant component of side-to-side shearing motion. As can be deduced from Figure 2-8, for upward wave incidence, the ground shaking in the S waves becomes both vertical and horizontal, which is the reason that the S wave motion is so effective in damaging structures.

The other two types of earthquake waves are called **surface waves** because their motion is restricted to near the earth's surface. Such waves are analogous to waves in the ocean that do not disturb the water at depth. In a similar way, as the depth below the ground surface increases, the ground displacements of seismic surface waves decrease.
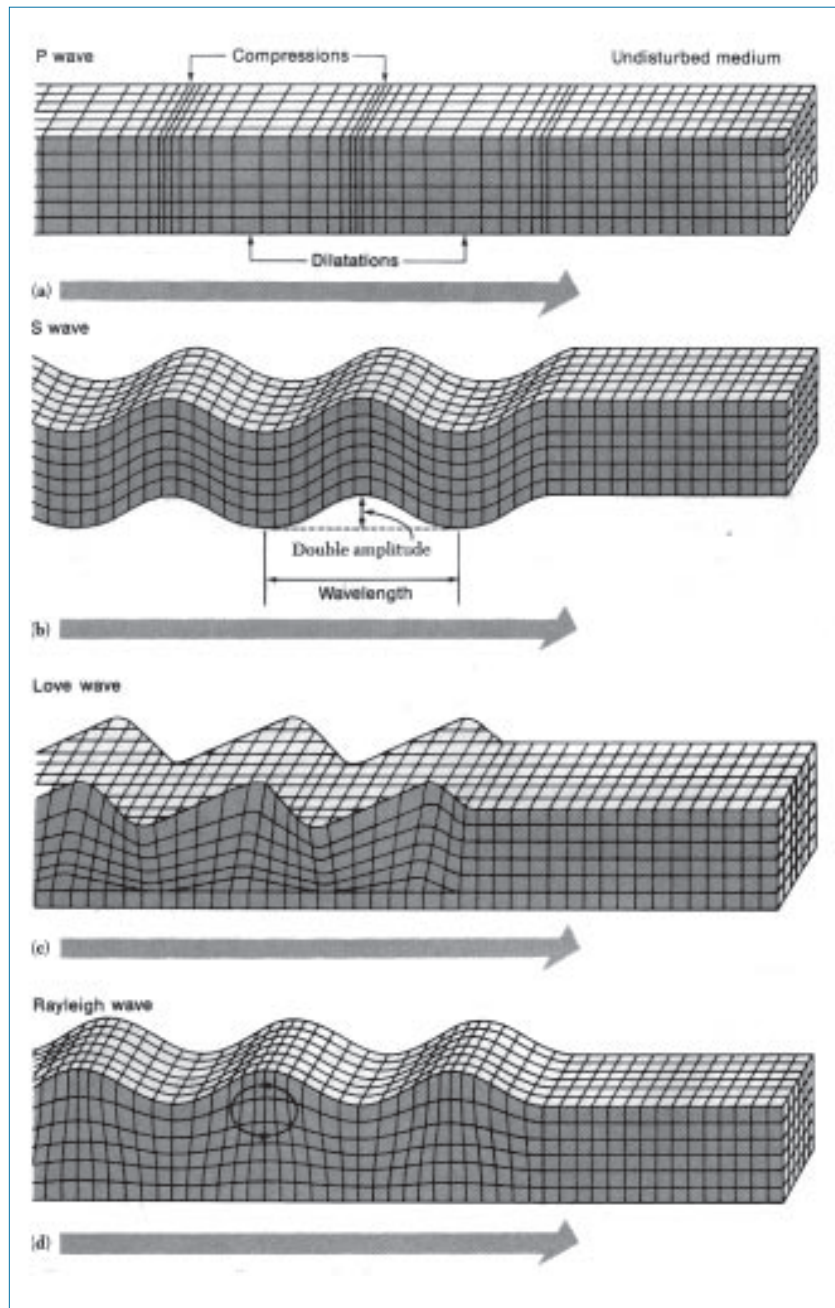
Figure 2-8: Diagram illustrating the forms of ground motion near the ground surface in four types of earthquake waves.

.

NATURE OF EARTHQUAKES AND SEISMIC HAZARDS

The first type of surface wave is called a **Love wave** (Figure 2-8c) Its motion is the same as that of S waves that have no vertical displacement; it moves the ground side to side in a horizontal plane parallel to the earth's surface, but at right angles to the direction of propagation. The second type of surface wave is called a **Rayleigh wave** (Figure 2-8d). Like ocean waves, the particles of rock displaced by a Rayleigh wave move both vertically and horizontally in a vertical plane oriented in the direction in which the waves are traveling. The motions are usually in a retrograde sense, as shown by the arrows in Figure 2-8. Each point in the rock moves in an ellipse as the wave passes.

Surface waves travel more slowly than P and S waves and Love waves travel faster than Rayleigh waves in the same geological formation. It follows that as the seismic waves radiate outwards from the rupturing fault into the surrounding rocks, the different types of waves separate out from one another in a predictable pattern. However, because large earthquake fault sources have significantly extended slip surfaces (i.e., many tens of kilometers), the separation is often obscured by overlapping waves of different wave types at sites close to the fault. Examples of near-fault large amplitude time histories are shown in Figure 2-9.

As seismic body waves (the P and S waves), move through layers of rock or soil, they are reflected or refracted at the layer interfaces. To complicate matters further, whenever either one is reflected or refracted, some of the energy of one type is converted to waves of the other type. When the material stiffnesses differ from one layer to another, the layers act as wave filters that amplify the waves at some frequencies and deamplify them at others.

It is important to note that when P and S waves reach the surface of the ground, most of their energy is reflected back into the crust, so that the surface is affected almost simultaneously by upward and downward moving waves. For this reason, considerable amplification of shaking typically occurs near the surface, sometimes doubling the amplitude of the upcoming waves. This surface amplification enhances the input shaking to structures and is responsible for much of the damage produced at the surface of the earth. In contrast, in many earthquakes, mineworkers below ground report less shaking than people on the surface. Nowadays, it is routine for soil engineers to make allowance for the wave amplification effect as the input seismic waves pass upwards through the soil layer to the ground surface.
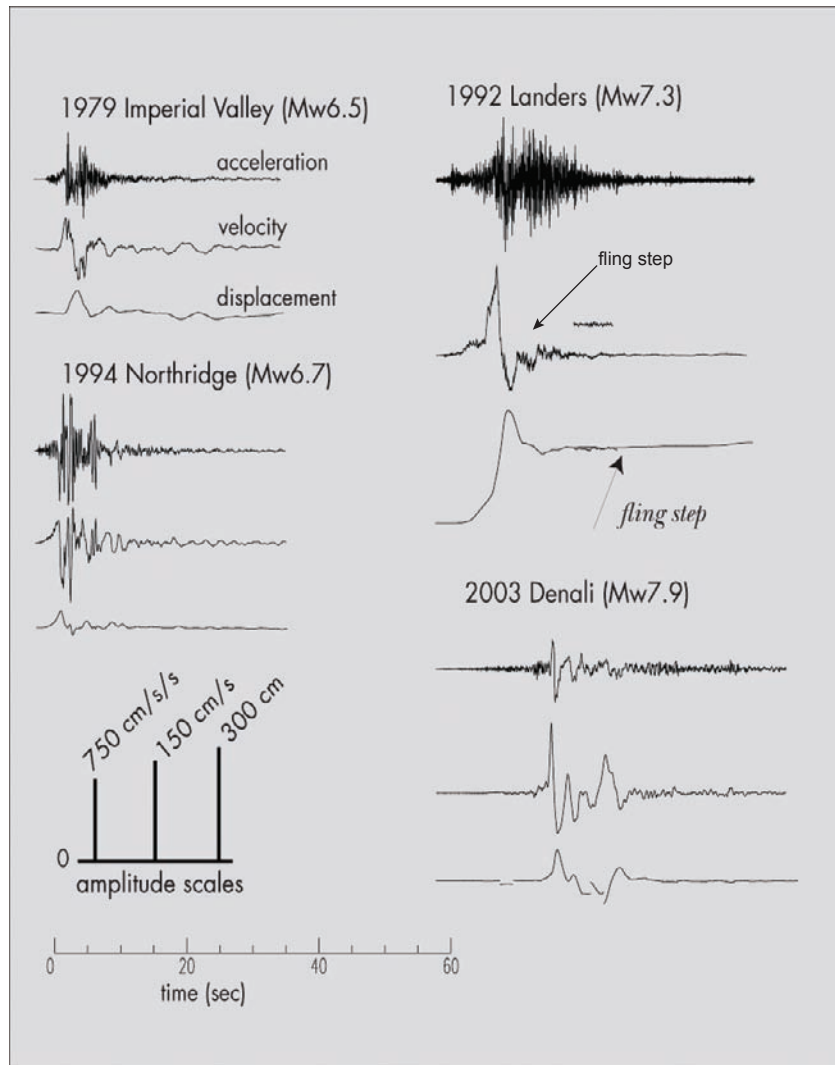
Figure 2-9: Examples of near-fault, large amplitude seismograms (time-histories).

The figure includes records from Imperial Valley, Landers (Lucerne), Northridge (Newhall) and Denali (Trans-Alaska Pipeline). Note the permanent offset in displacement of the Landers record. This is due to fault ground rebound or fling, shown by the arrows. The bars (lower left) give the common amplitude scales for the displacement, velocity and acceleration records.

It should be noted that seismic S waves travel through the rocks and soils of the earth with both a shearing and a rotational component. The latter components of ground motion have important effects on the response of certain types of structures, and some building codes now take rotational ground motion into consideration.

Seismic waves of all types progressively decrease in amplitude with distance from the source. This attenuation of waves varies with different regions in the United States. The attenuation of S waves is greater than that of P waves, but for both types attenuation increases as wave frequency increases. Ground motion attenuation can flatten and even reverse its downward trend due to strong reflected arrivals from rock interfaces. It has been shown that such reflections led to elevated ground motions in the 60-80 km distance range from the 1989 Loma Prieta, California, earthquake (i.e., in Oakland and San Francisco). Deposits of low velocity sediments in geological basins can also cause elevated levels of ground motions.

For a more detailed discussion of seismic wave attenuation and theoretical wave amplitude, see Section 2.6.1.

The physical characteristics of seismic waves have been verified by many recordings at moderate (15-30 km) to larger distances from the wave source called the **far-field**, but are not adequate to explain important details of the heavy shaking near the source of an energetic earthquake called the **near-field**. As explained above, near a rupturing fault, the strong ground shaking consists of mixtures of seismic wave types that have not separated distinctly. Although this complication makes identification of P, S, and surface waves on strong motion records obtained near the rupturing fault difficult, there has been recent progress in this skill, based on correlations between actual recordings and theoretical modelling. This advance has made possible the computation of realistic ground motions at specified sites for engineering design purposes.

Three final points about seismic waves are worth emphasizing here:

❍ Earthquake waves are much affected by soil elastic properties. For example, in weathered surface rocks, alluvium and water-saturated soil, the relative sizes of P, S, and surface waves can vary significantly, depending on wave frequency, as they propagate through the

surficial non-homogenous geological structures. Under extreme conditions of large wave amplitude and special geotechnical properties, the linear elastic behavior breaks down and nonlinear effects occur.

❍ Patterns of incoming seismic waves are modified by the three-dimensional nature of the underground geological structures. As mentioned above, instrumental evidence on this effect was obtained from recordings of the 1989 Loma Prieta, California, earthquake. In this case, strong-motion recordings indicated that there were reflections of high-frequency S-waves from the base of the earth's crust at a depth of about 25 km under the southern San Francisco Bay. Also, in this earthquake, large differences in the rock structure from one side of the San Andreas fault to the other produced variations in ground motion by lateral refraction of S waves. The effect produced significant S wave amplitude variation as a function of azimuth from the seismic source, in a period range of about 1 to 2 seconds. In addition, there was measurable scattering of S waves by separate alluvial basins in the south part of San Francisco Bay. Overall, the seismic intensity was enhanced in a region between San Francisco and Oakland, about 10 km wide by 15 km long. The observed damage and seismic intensity are well explained by these seismological results.

❍ It is important to explain the special seismic intensity enhancement in the near field of the earthquake source. Because of special features of engineering importance, this discussion of seismic wave patterns near to the fault source is given in the separate Section 2.4. As may be seen in Figure 2-10, time histories of the seismic waves contain pulse-like patterns of motion of crucial importance to earthquake response of larger structures.

2.4. SEISMIC SOURCES AND STRONG MOTION

As has been discussed in the previous sections, seismic waves are generally generated by the sudden rupture of faults, but can also be initiated by other natural processes, such as pulsing of volcanic magma and landsliding. They can also be caused by man-made explosions and collapse of subterranean mines. The strength of S-wave radiation depends upon the mechanism of the source. In particular, fault rupture is an efficient generator of S waves, which are responsible for much of the demand of earthquakes on the built environment. The seismic wave amplitudes vary

with azimuth from the source as a result of the orientation of the force couples that cause the fault rupture. The resulting pattern of radiation of all types of seismic waves may be described mathematically using the same terms used in defining the different types of faults (see Figure 2-3), i.e., in terms of the fault strike, dip, and direction of slip.

2.4.1 Earthquake Magnitude

The original instrumental measure of earthquake size has been significantly extended and improved in recent years. First, because the fundamental period of the now superseded Wood-Anderson seismograph is about 0.8 sec., it selectively amplifies those seismic waves with periods ranging from 0.5 to 1.5 sec. It follows that because the natural periods of many building structures are within this range, the first commonly used parameter, called the **Richter magnitude** (M_L) based on this seismograph, remains of value to architects. Generally, shallow earthquakes have to attain Richter magnitudes of more than 5.5 before significant damage occurs, even near the source of the waves. It should be remembered that a one unit increase in magnitude indicates a tenfold increase in the amplitude of the earthquake waves.

The definition of all magnitude scales entails that they have no theoretical upper or lower limits. However, the size (i.e., the seismic moment) of an earthquake is practically limited at the upper end by the strength of the rocks of the earth's crust and by the area of the crucially strained fault source. Since 1935, only a few earthquakes have been recorded on seismographs that have had a magnitude over 8.0 (see Table 2-1). At the lower extreme, highly sensitive seismographs can record earthquakes with a magnitude of less than minus two.
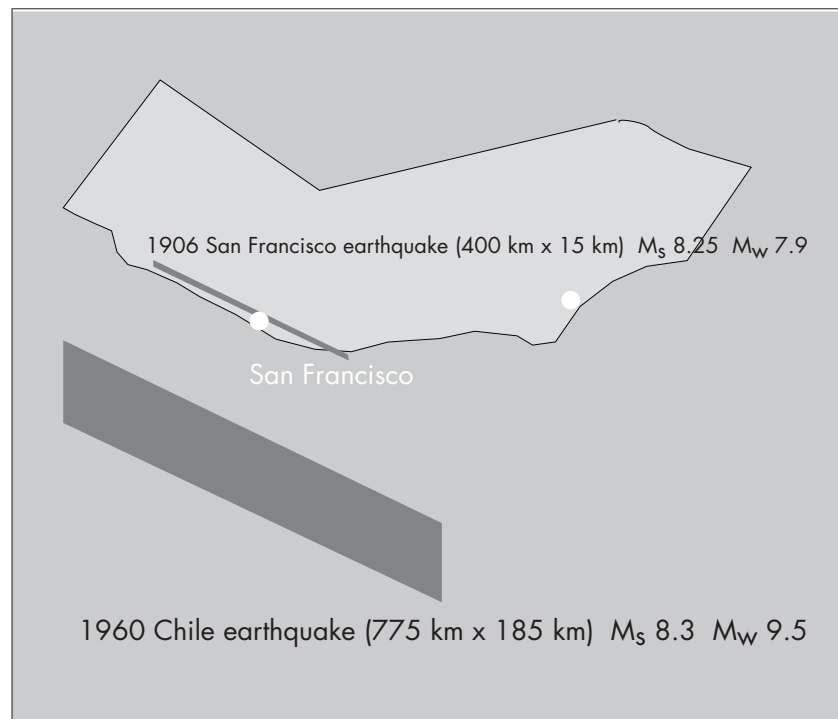
For reference, an architect may still encounter the following magnitude scales.

❍ **Surface Wave Magnitude** (M_S) is based on measuring the amplitude of surface waves with a period of 20 sec. Surface waves with a period around 20 sec are often dominant on the seismograph records of distant earthquakes (epicentral distances of more than 1,000 km).

❍ **Body Wave Magnitude** (M_b) Because deep focus earthquakes have no trains of surface waves, only the amplitude of the recorded P wave is used.

Nowadays, because of the shortcomings of M_L, M_b, and to a lesser degree M_s in distinguishing between the size of the biggest earthquakes, the **Moment Magnitude** scale, M_W , has replaced earlier definitions.

Studies have shown that the Richter Magnitude (M_L) scale progressively underestimates the strength of earthquakes produced by large fault ruptures. The upper-bound value for this scale is about $M_L = 7$. The body wave magnitude (M_b) saturates at about the same point. In contrast, the surface-wave magnitude (M_s) that uses the amplitude of waves with periods of 20 seconds saturates at about $M_s = 8$. Its inadequacy in measuring the size of great earthquakes can be illustrated by comparing values for the San Francisco earthquake of 1906 and the great Chilean

Figure 2-10: Two earthquakes may have equal magnitudes but be distinctly unequal in other respects.

1906 San Francisco earthquake (400 km x 15 km) M_s 8.25 M_W 7.9

San Francisco

1960 Chile earthquake (775 km x 185 km) M_s 8.3 M_W 9.5

The 1906 San Francisco, California, earthquake ruptured rock over a shorter length and shallower depth - only about 1/25 the area - as the 1960 Chilean earthquake. Although the surface wave magnitudes are the same, the moment magnitude for these two earthquakes (Table 2-1) are distinctly different. A sketch of the outline of California is shown for scale.

NATURE OF EARTHQUAKES AND SEISMIC HAZARDS

earthquake of 1960. Both earthquakes had a surface wave magnitude (M_S) of 8.3. However, the area that ruptured in the San Francisco earthquake was approximately 15 km deep and 400 km long, whereas the length that ruptured in the Chilean earthquake was equal to about half of the state of California. Clearly the Chilean earthquake was a much "larger" event (Figure 2-10).

The moment-magnitude scale (M_W) does not suffer from saturation for great earthquakes. The reason is that it is directly based on the forces that work over the area of the fault rupture to produce the earthquake and not on the amplitude and limited frequencies of specific types of seismic waves. Hence, as can be expected, when moment magnitudes were assigned to the 1906 San Francisco earthquake and the 1960 Chilean earthquake, the magnitude of the San Francisco earthquake dropped to 7.9, whereas the magnitude of the Chilean earthquake rose to 9.5. M_S and M_W for some great earthquakes are compared in Table 2-1.

2.4.2 Elastic Rebound and its Relationship to Earthquake Strong Ground Motion

The slip along the San Andreas fault that produced the 1906 earthquake was studied by H. F. Reid. He imagined a bird's-eye view of a straight line drawn at a certain time at right angles across the San Andreas fault. As the tectonic force slowly works, the line bends, the left side shifting in relation to the right. The deformation amounts to about a meter in the course of 50 years or so. This straining cannot continue indefinitely; sooner or later the weakest rocks, or those at the point of greatest strain, break. This fracture is followed by a springing back or **rebounding**, on each side of the fracture.

This **elastic rebound** was believed by Reid to be the immediate cause of earthquakes, and his explanation has been confirmed over the years. Like a watch spring that is wound tighter and tighter, the more the crustal rocks are elastically strained, the more energy they store. When a fault ruptures, the elastic energy stored in the rocks is released, partly as heat and partly as elastic waves. These waves are the earthquake. A remarkable example of this phenomenon that produced striking offsets occurred in Turkey in the 1999 Izmit earthquake (Figure 2-4).

Straining of rocks in the vertical dimension is also common. The elastic rebound occurs along dipping fault surfaces, causing vertical disruption

Table 2-1: Magnitudes of some great earthquakes

Date	Region	M_S	M_W
January 9, 1905	Mongolia	8.25	8.4
January 31, 1906	Ecuador	8.6	8.8
April 18, 1906	San Francisco	8.25	7.9
January 3, 1911	Turkestan	8.4	7.7
December 16, 1920	Kansu, China	8.5	7.8
September 1, 1923	Kanto, Japan	8.2	7.9
March 2, 1933	Sanrika	8.5	8.4
May 24, 1940	Peru	8.0	8.2
April 6, 1943	Chile	7.9	8.2
August 15, 1950	Assam	8.6	8.6
November 4, 1952	Kamchatka	8	9.0
March 9, 1957	Aleutian Islands	8	9.1
November 6, 1958	Kurile Islands	8.7	8.3
May 22, 1960	Chile	8.3	9.5
March 28, 1964	Alaska	8.4	9.2
October 17, 1966	Peru	7.5	8.1
August 11, 1969	Kurile Islands	7.8	8.2
October 3, 1974	Peru	7.6	8.1
July 27, 1976	China	8.0	7.5
August 16, 1976	Mindanao	8.2	8.1
March 3, 1985	Chile	7.8	7.5
September 19, 1985	Mexico	8.1	8.0
September 21, 1999	Taiwan	7.7	7.6
November 2, 2002	Alaska	7.0	7.9
December 26, 2004	Sumatra	NA	9.0

NATURE OF EARTHQUAKES AND SEISMIC HAZARDS

in level lines at the surface and fault scarps. Vertical ground displacement too can amount to meters in dip-slip faulting (as in the 1999 Chi Chi, Taiwan, earthquake, faulting in Figure 2-5).

Observations show that fault displacement occurs over a continuum of rates from less than a second to very slow fault slip. Although the latter "creep" can pose significant hazard for structures built across such rupturing faults, these slow slips do not radiate elastic seismic waves. Indeed, the generation of strong seismic waves requires that the elastic rebound of the fault is rapid. The Lucerne record (Figure 2-9) for the Landers earthquake 3 km from the fault shows that elastic rebound (**fling-step**) occurred over about 7 seconds. This static offset arises from near-field waves and their amplitudes attenuate more rapidly than far-field body waves. Since this attenuation is strong, and the rise time of the fling-step increases with distance, large dynamic motions derived from this phenomenon are typically limited to sites very close to the fault. A time derivative of the fling-step produces a pulse-like velocity record (Figure 2-10). For example the fling-step at the Lucerne site for the Landers earthquake was recorded 3 km from the fault trace, and the 3 m/s peak velocity recorded within 1 km of the fault for the 1999 Chi-Chi, Taiwan, earthquake (Table 2-2) had a significant contribution from the fling-step.

2.4.3 Source Directivity and its Effect on Strong Ground Motions

For structures near active faults an additional seismological source effect may be important in design in which the direction and speed of a rupture along a fault focuses wave energy, producing direction-dependent seismic wave amplitudes. This direction-dependent amplitude variation called **directivity** affects the intensity and damage potential of strong ground motions near and at moderate distances from the fault source. In contrast to large pulse-like dynamic motions derived from a fling-step, those due to directivity are results of the superposition or focusing of far-field body waves. Since waves distant from the fault attenuate less with distance than those nearby, directivity pulses with elevated motions can occur some distance from the fault. To keep these two effects separate, the terms "**directivity pulse**" and "**fling-step**" have been used for the rupture directivity and elastic rebound effects, respectively.

Directivity is a term that describes the focusing and defocusing of waves due to the direction of rupture with respect to the direction to a given site. Therefore it describes azimuthal variation in earthquake ground

motion about the fault. The difference between the rupture direction and the direction to the site is related by an angle. Large ground accelerations and velocities are associated with small angles, since a significant portion of the seismic energy is channeled in the direction to the site. Consequently, when a large urban area is located within the small angle, it will experience severe damage. Studies show that in the Northridge earthquake of 1994, the rupture propagated in the direction opposite from downtown Los Angeles and the San Fernando Valley, causing only moderate damage, whereas the collapsed SR-18/I5 highway interchange was in an area of small angle. In the Kobe, Japan, earthquake of 1995, the rupture was directed towards the city of Kobe, resulting in severe damage. The stations that lie in the direction of the earthquake rupture propagation will record shorter strong-motion duration than those located opposite to the direction of propagation.

Directivity can significantly affect strong ground motion by as much as a factor of 10, and methods are being developed to account for this effect through numerical simulation of earthquake ground motions, and by empirical adjustment of ground motion attenuation relationships. However, it is not clear how to incorporate directivity into methods for predicting ground motion in future earthquakes, because the angle between the direction of rupture propagation and the source to recording site and the slip history on the fault is not known before the earthquake. Studies that incorporate directivity in the analysis must therefore investigate many rupture scenarios to examine the range of possible motions.

2.5 STRONG GROUND MOTION

As mentioned earlier, for architectural purposes it is important to know that near-fault ground motions often contain significant **velocity wave pulses**, which may be from fling in the near-fault, fault-parallel direction, or from directivity in the fault-normal direction extending a considerable distance from the ruptured fault. For strike-slip fault sources, they dominate the horizontal motion and may appear as single or double pulses, each with single or double-sided amplitudes. The duration (period) of the main pulse may range from 0.5 sec. to 5 sec. or more for the greatest magnitudes. These properties depend on the type, length, and complexity of the fault rupture.

NATURE OF EARTHQUAKES AND SEISMIC HAZARDS

2.5.1 Duration of Strong Shaking

Field studies demonstrate that the duration of strong ground shaking is often a critical factor in the response of foundation materials and structures. There is no way to determine the duration of a design event and factor duration into current design codes. Soil response in particular can be strongly dependent on the increases in pore water pressure with repeated cyclic input. Also nonlinear degradation of damaged structures (also caused by long shaking and in large aftershocks) can lead to collapse.

2.5.2 Estimating Time Histories

Numerical modeling can be particularly helpful in predicting the effect of certain special geological structures on a hazard at a site. Consider, for example, the response of the Los Angeles alluvial basin to a large earthquake from slip of the San Andreas fault. A computer simulation was made in 1995 by Olsen et al. that gives wave motion for a three-dimensional numerical model, when the source is a magnitude 7.75 earthquake along the 170 km section of the San Andreas fault between Fort Tejon Pass and San Bernardino. The results are graphed in Figure 2-11. The wave propagation is represented as horizontal velocities of the ground parallel to the San Andreas fault.

The snapshots show that after 40 sec., ground motion in the basin begins to intensify, and 10 sec later the entire Los Angeles basin is responding to large amplitude surface waves. (The waves shown are spectrally limited to frequencies below 0.4 Hz. In an actual earthquake, the ground motions would contain much higher frequencies, but the effects would be similar.) The component of motion perpendicular to the fault strike is 25% larger than the parallel component near the fault due to the directivity of the rupture (see Section 2.4.2). This simulation predicted long-period peak ground velocities greater than 1 m/sec. at some areas in Los Angeles, even though the main trough of the basin is about 60 km from the fault. Later analysis of the same region suggests that such computed amplitude factors (up to six in deeper parts of the basin) should be used by planners and designers as a guide only and with caution.

Instead of such synthetic models, quasi-empirical seismic strong ground motions, based on modified actual recordings of similar earthquakes, are now normally used to estimate seismic hazard. Two equivalent representations of the hazard are commonly considered together. The first is an
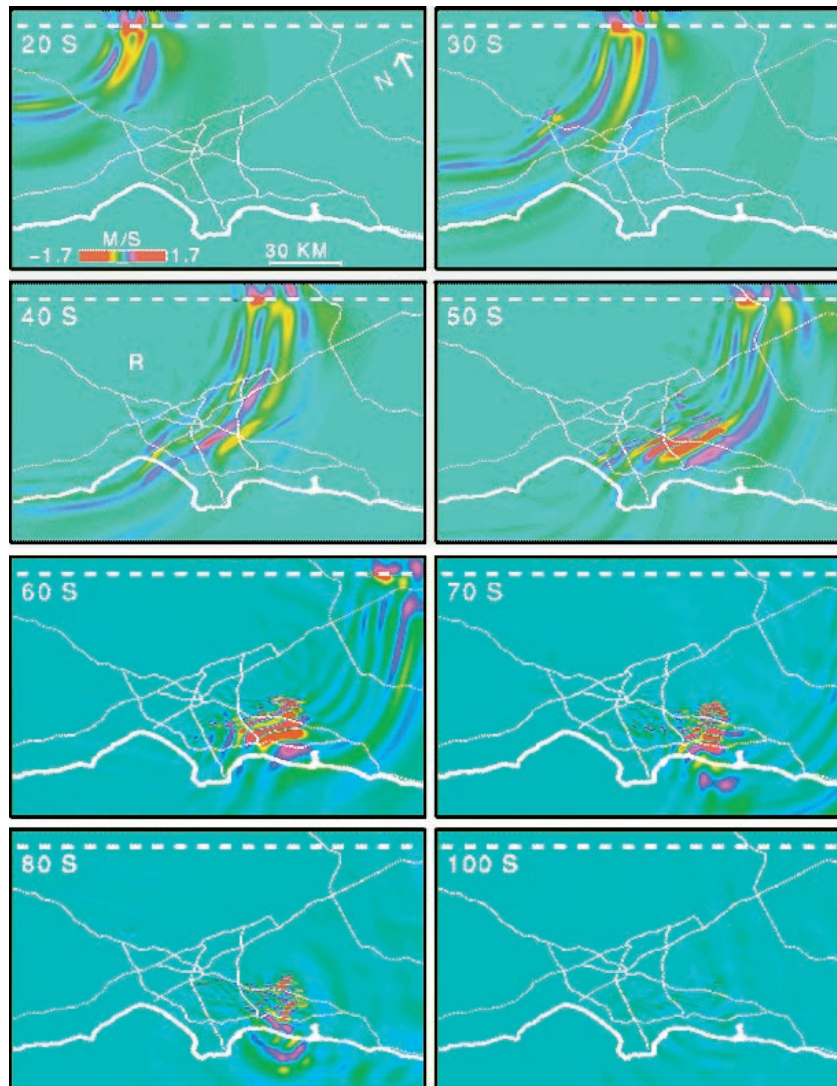
Figure 2-11: Aerial snapshots of a simulated wave propagation in the Los Angeles area.

The snapshots depict velocities from 20 s to 100 s after the origin time of the rupture. Red depicts large amplitudes of both positive and negative polarity. R depicts the initiation of an area of local resonance above the deepest part of the San Fernando basin. The particle motion is scaled by a constant for all snapshots.

SOURCE: OLSEN ET AL. (1995) FOR A HYPOTHETICAL SAN ANDREAS FAULT EARTHQUAKE

NATURE OF EARTHQUAKES AND SEISMIC HAZARDS

estimate of the **time-history** of the ground motion appropriate to the site. The second is the **response spectra** (the spectral response of a damped single degree-of-freedom harmonic oscillator, see section 4.5.2) for the whole seismic motion at the site. These two representations of seismic hazard can be connected by appropriate transformations between the time and frequency descriptions of the earthquake.

In the simplest time-history representation, the major interest of architects and engineers in assessing the earthquake risk has traditionally been in the peak ground acceleration (PGA), velocity, and displacement as a function of frequency, or period. In recent work related to large and critical engineered structures, however, the pattern of wave motion has been recognized as crucial in structural response, because the nonlinear response of such structures is often dependent on the sequence of arrival of the various types of waves. In other words, damage would be different if the ground motion were run backwards rather than in the actual time sequence of arrival. The sequence (phasing) of the various wave types on the artificial seismograms can be checked from seismological knowledge of times of arrival of the P, S, directivity-pulse, fling, and surface waves. Only in this way can a realistic envelope of amplitudes in the time histories be assumed.

In the usual calculation, the initial step is to define, from geological and seismological information, the fault sources that are appropriate and dangerous for the site of interest. This fault source selection may be largely deterministic, based on prior experience, or largely probabilistic, and may be decided on grounds of acceptable risk. Next, specification of the propagation path of the strongest waves is made, as well as the P, S and surface wave velocities along the path. These speeds allow calculation of the appropriate delays in wave propagation between the source and the multi-support points of the structure and the angles of approach of the incident seismic waves.

The computation of realistic motions then proceeds as a series of nonlinear iterations, starting with the most appropriate observed strong-motion record available, called the seed motion, to a set of more specific time histories, which incorporate the seismologically defined wave patterns. The seed strong-motion accelerograms are chosen to approximate the seismic source type (dip-slip, etc.) and geological specifications for the region in question. (A set of suggested time histories

for seed motions is listed in Table 2-2). Many sample digitized records can be downloaded using the Virtual Data Center (VDC) website of the Consortium of Organizations for Strong-Motion Observational Systems (COSMOS) (see section 2.10). The frequency content of the desired time-history is controlled by applying engineering constraints, such as a selected response amplitude spectrum. Such target spectra are obtained, for example, from previous engineering analysis and from earthquake building codes (see, e.g., IBC, 2003).

2.6. SEISMIC HAZARD

2.6.1 Empirical Attenuation Curves

As has been outlined in the previous sections, the estimation of the earthquake hazard in a region or at a site requires the prediction of ground motions. The empirical estimation of seismic hazard curves is a necessary step. It follows that hazard calculations involve a number of assumptions and extrapolations. The common initial difficulty is ignorance of the actual seismic wave attenuation for the site in question, despite the recent publication of a variety of average curves for certain regions. The importance of attenuation factors in calculation of predicted ground motion at arbitrary distances has led to competing empirical attenuation forms based on available intensity measurements and geological knowledge.

Usually wave attenuation changes significantly from one geological province to another, and local regional studies are advisable to calibrate the parameters involved.

As mentioned in Section 2.4, although different measures of earthquake magnitude are still used, particularly with historical data, the moment magnitude (M_w) is now usually adopted as a standard measure of size in attenuation statistics. Also, nowadays, some form of "closest" distance to the rupture is used as the distance parameter rather than epicentral or hypocentral distance. It is important to use the appropriate distance measure for a given attenuation relation. The most common source, ray path, and site parameters are magnitude, distance, style-of-fault, directivity, and site classification. Rupture directivity is defined in detail in Section 2.4.3 and is not discussed here. In some studies, additional parameters are used: hanging-wall flag, rupture directivity parameters, focal depth, and soil depth classification.

NATURE OF EARTHQUAKES AND SEISMIC HAZARDS

Table 2-2: Examples of near-fault strong-motion recordings from crustal earthquakes with large peak horizontal ground motions

Earthquake	Magnitude M_W	Source Mechanism	Distance km*	Acceleration (g)	Velocity (cm/sec)	Displace (cm)
1940 Imperial Valley (El Centro, 270)	7.0	Strike-Slip	8	0.22	30	24
1971 San Fernando (Pacoima 164)	6.7	Thrust	3	1.23	113	36
1979 Imperial Valley (EC #8, 140)	6.5	Strike-Slip	8	0.60	54	32
Erzican (Erzican, 1992)	6.9	Strike-Slip	2	0.52	84	27
1989 Loma Prieta (Los Gatos, 000)	6.9	Oblique	5	0.56	95	41
1992 Lander (Lucerne, 260)	7.3	Strike-Slip	1	0.73	147	63
1992 Cape Mendocino (Cape Mendocino, 000)	7.1	Thrust	9	1.50	127	4
1994 Northridge (Rinaldi, 228)	6.7	Thrust	3	0.84	166	29
1995 Kobe (Takatori, 000)	6.9	Strike-Slip	1	0.61	127	36
1999 Kocaeli (SKR, 090)	7.4	Strike-Slip	3	0.41	80	205
1999 Chi-Chi (TCU068, 000)	7.6	Thrust	1	0.38	306	940

* distence km shows surface distance from fault

There are also differences in site classification schemes in different regions that make comparison of estimates of ground motions from alternative estimates difficult. Broad site categories such as "rock," "stiff-soil," and "soft-soil" are common and affect ground motions (Figure 2-12), but more quantitative site classifications based on the S-wave velocity, such as the average S-wave speed in the top 30 m, are now preferred. Most attenuation relations simply use a site category such as "deep soil"; however, this general category covers a wide range of soil depths from less than 100 m to several kilometers of sediments. Some attenuation relations use an additional site parameter to describe the depth of the sediment.

For thrust faults, high-frequency ground motions on the upthrown block (hanging-wall side of a thrust fault) are much larger than on the downdropped block (footwall). This increase in ground motions on the hanging wall side is in part an artifact of using a rupture distance measure, but may also be due to the dynamics of waves interacting with the dipping fault plane and the surface of the earth. If a site on the hanging wall and footwall are at the same rupture distance, the site on the hanging wall side is closer to more of the fault than the site on the footwall side. Such difference was marked in damage patterns to houses and other structures in the 1999 Chi Chi, Taiwan, earthquake ($M_W = 7.6$).

In the eastern U.S., incorporation of a variation in the distance slope of the attenuation relation to accommodate the increase in ground motions due to supercritical reflections from the base of the crust has been suggested. Typically, this result leads to a flattening of the attenuation curve at distances of about 100 km). This is most significant for regions in which the high activity sources are at a large distance from the site.
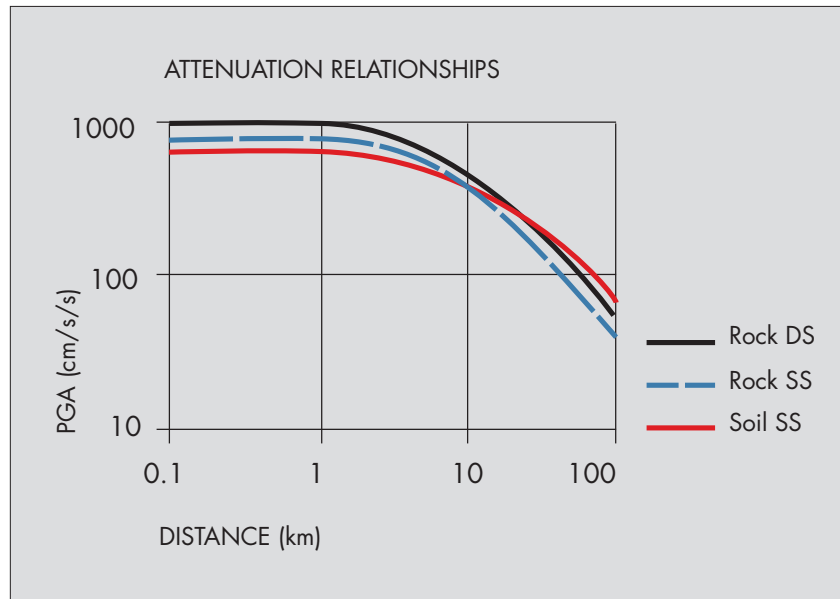

Figure 2-12: Examples of attenuation curves for a M_W7 earthquake obtained by data regression, illustrating the effects of a **site** type: rock (blue dashed) vs. deep soil (red), and **event** type: strike-slip fault (blue dashed) vs. reverse fault (black)

SOURCE: ABRAHAMSON AND SILVA, 1997

NATURE OF EARTHQUAKES AND SEISMIC HAZARDS

An important statistical issue in developing attenuation relations is the uneven sampling of the data from different earthquakes. For example, in some cases, an earthquake may have only one or two recordings (e.g., the 1940 El Centro event), whereas, some of the recent earthquakes have hundreds of recordings (e.g., the 1999 Chi Chi earthquake). The use of statistical weights can reduce this uneven sampling problem. There are two extremes: give equal weight to each data point or give equal weight to each earthquake. The random-effects model seems best. It uses a weighting scheme that varies between giving equal weight to each earthquake and equal weight to each data point, depending on the distribution of the data.

In addition to the median measure of ground motion, the standard deviation of the measured ground motion parameters is also important for either deterministic or probabilistic hazard analyses. Worldwide, it is common to use a constant standard deviation, but recently, several attenuation relations have attributed magnitude or amplitude dependence to the standard deviation.

2.6.2 Probabilistic Seismic Hazard Analysis (PSHA) and Building Codes

Probabilistic Seismic Hazard Analysis provides an estimate of the likelihood of hazard from earthquakes based on geological and seismological studies. It is probabilistic in the sense that the analysis takes into consideration the uncertainties in the size and location of earthquakes and the resulting ground motions that could affect a particular site. Seismic hazard is sometimes described as the probability of occurrence of some particular earthquake characteristic (such as peak ground acceleration) For statistical reasons, these probabilities cover a range of values, and because risk involves values being greater than expected, the word "exceedance" has been coined as explained below.

Probabilistic analysis uses four basic steps in order to characterize the probable seismic hazard:

● Identification of the seismic source or faults.

This often includes the identification of surface faulting features that can be recognized as active. Seismic sources may be specified as site specific, for an active source region or, when geologic information is poor,

for random occurrence of active faults in the study region. Once the faulting hazard is identified, earthquake occurrence statistics are compiled, which might be in the form of annual rates of seismic events or, in an active regions of known faults, more specific information provided by paleoseismic studies such as dating episodes of fault offsets. (Paleoseismology involves digging to expose the underground face of a fault, so that historic offsets can be made visible and material suitable for radiocarbon age dating can be obtained). The objective is to obtain a measure of the frequency of earthquakes within a given time period as a function of magnitude that may be expressed as a probabilistic statement (or mathematical likelihood) of the earthquake occurrence.

● **Characterization of annual rates of seismic events.**

As an example, if there is one magnitude 7 earthquake in a given region every 50 years, then the annual rate of occurrence is 0.5. Commonly used maps to express probability are cast in terms of a 50-year return period, and are used to determine the ground motion values to be specified in building codes and used in seismic design.

Since damaging ground motions can result from nearby moderate earthquakes as well as large distant earthquakes, the recurrence rates for each magnitude range must be determined.

● **Development of attenuation relationships**

Attenuation relationships and their uncertainty due to limited information must be developed so that the ground motion parameters for each of the sources developed in the first step can be related to the distance of the study site from them.

● **Combining factors**

The annual recurrence and the attenuation are combined to determine the site-specific hazard.

Until the 1990s, seismic building codes used a single map of the United States that divided the country into numbered seismic zones (0,1,2,3,4) in which each zone was assigned a single acceleration value in % g which was used to determine seismic loads on the structure.

Starting in the 1970s, new hazard maps began to be developed on a probabilistic basis. In the 1994 *NEHRP Recommended Provisions* (FEMA 222A), two maps of the US were provided in an appendix for comment. They showed effective peak acceleration coefficients and effective peak velocity–related coefficients by use of contour lines that designated regions of equal value. The ground motions were based on estimated probabilities of 10% of exceedance in various exposure times (50, 100 and 250 years). The 1997 *Recommended Provisions* (FEMA 302) provided the first spectral response maps to pass consensus ballot. This lead to the current maps which, with some revisions, are now used in the 2003 *NEHRP Provisions* (FEMA 450), the ASCE *Prestandard and Commentary for the Seismic Rehabilitation of Buildings* (FEMA 356), and the *International Building Code.*

The probabilistic analysis is typically represented in maps in the form of a percentage probability of exceedance in a specified number of years. For example, commonly used probabilities are a 10% probability of exceedance in 50 years (a return period of about 475 years) and a 2% probability of exceedance in 50 years (a return period of about 2,500 years). These maps show ground motions that may be equaled but are not expected to be exceeded in the next 50 years: the odds that they will not be exceeded are 90% and 98%, respectively.

Seismic hazard probability maps are produced by the United States Geological Survey (USGS) as part of the National Seismic Hazard Mapping Project in Golden, Colorado. The latest sets of USGS of maps provide a variety of maps for Peak Ground Acceleration and Spectral Acceleration, with explanatory material, and are available on the USGS web site

The USGS map shown in Figure 2-13 is a probabilistic representation of hazard for the coterminous United States. This shows the spectral acceleration in %g with a 2% probability of exceedance in 50 years: this degree of probability is the basis of the maps used in the building codes.

The return period of 1 in 2,500 years may seem very infrequent, but this is a statistical value, not a prediction, so some earthquakes will occur much sooner and some much later. The design dilemma is that if a more frequent earthquake - for example, the return period of 475 years - were used in the lower seismic regions, the difference between the high and low-probability earthquakes is a ratio of between 2 and 5. Design for
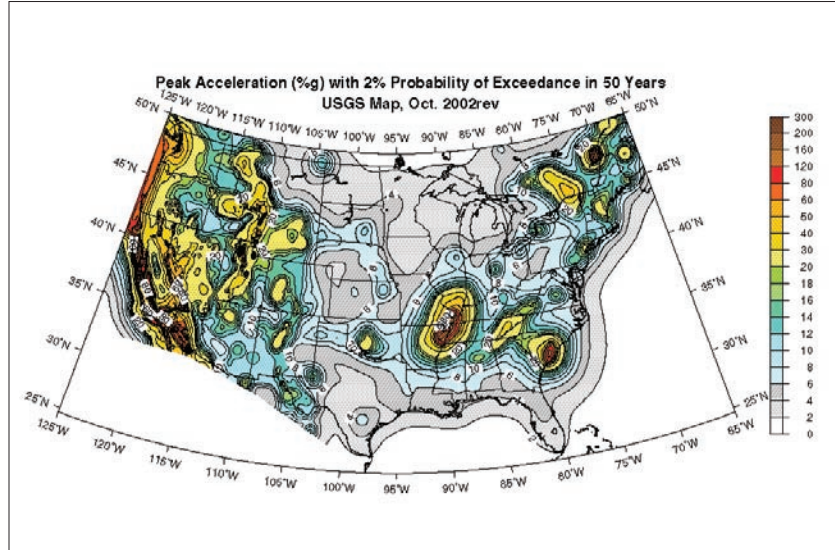
Figure 2-13: Spectral Acceleration values in %g with a 2% Probability of Exceedance in 50 years for the coterminous United States. The color scale to the right relates to the %g values.

SOURCE: USGS NATIONAL SEISMIC HAZARD MAPPING PROJECT

the high-probability earthquake would be largely ineffective when the low-probability event occurred

In practical terms, the building designer must assume that the large earthquake may occur at any time. Thus, use of the 2,500 return period earthquake in the lower seismic regions ensures protection against rare earthquakes, such as the recurrence of the 1811-1812 earthquake sequence in New Madrid, Missouri, or the 1898 Charleston, South Carolina, earthquake. It was judged that the selection of 2 per cent in 50 years likelihood as the maximum considered earthquake ground motion would result in acceptable levels of seismic safety for the nation.

The acceleration experienced by a building will vary depending on the period of the building, and in general short-period buildings will experience more accelerations than long-period buildings, as shown in the response spectrum discussed in section 4.5.3. The USGS maps recognize this phenomenon by providing acceleration values for periods

NATURE OF EARTHQUAKES AND SEISMIC HAZARDS

of 0.2 seconds (short) and 1.0 seconds (long). These are referred to as spectral acceleration (SA), and the values are approximately what are experienced by a building (as distinct from the peak acceleration which is experienced at the ground). The spectral acceleration is usually considerably more than the peak ground accelerations, for reasons explained in Section 4.7.

Figure 2-14 shows 2%/50 year probability maps for the central and southern United States for 0.2 seconds, and Figure 2-15 shows a similar map for 1.0 second spectral acceleration.

These USGS probability maps provide the basis for USGS maps used in building codes that provide design values for spectral acceleration used by structural engineers to calculate the seismic forces on a structure. These design value maps differ by use of a maximum considered earthquake (MCE) for the regions. For most regions of the country the maximum considered earthquake is defined as ground motion with a uniform likelihood of exceedance of 2% in 50 years (a return period of about 2,500 years) and is identical to the USGS probability maps. However, in regions of high seismicity, such as coastal California, the seismic hazard is typically controlled by large-magnitude events occurring on a limited number of well-defined fault systems. For these regions, rather than using the 2% in 50-year likelihood, it is considered more appropriate to directly determine the MCE ground motions based on the characteristic earthquakes of those defined faults.

The 2000 *NEHRP Provisions* and the 2003 *IBC* provide maps that show the MCE for the Coterminous United States, California and Hawaii, the Utah region, Alaska, the Puerto Rico region and Guam. These maps are produced in black and white line with no color coding. A CD-ROM is available from FEMA, USGS, ACSF and IBC that includes a software package that can provide map values based on latitude/longitute or postal zip code.

Finally, the acceleration values shown on the maps are not used directly for design. Instead, they are reduced by 1/3; this value is termed the Design Earthquake (DE) and is the value used by engineers for design. The reason for this is that engineers believe that the design provisions contain at least a margin of 1.5 against structural failure. MCE is inferred to
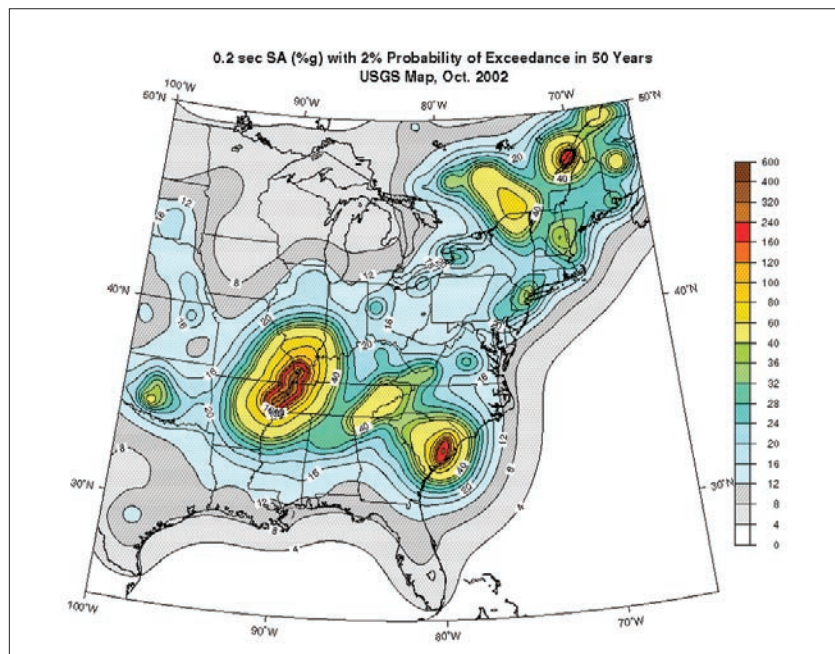
Figure 2-14: 0.2 second (short) period Spectral Acceleration values in %g with a 2% Probability of Exceedance in 50 years for Central and Southern United States.

SOURCE: USGS NATIONAL SEISMIC HAZARD MAPPING PROJECT

provide collapse prevention level, while the actual design is done using the design earthquake (DE), which is 2/3 MCE for code-level life-safety protection-level. This belief is the result of the study of the performance of many types of buildings in earthquakes, mostly in California.

There have been numerous comments that the level of seismic hazard being used in the central and eastern United States results in design values that are unreasonably high. As a result, a review and re-verification of the 2% in 50 years ground-shaking probability for use as the MCE will be implimented. This study is being done as part of the 2008 *NEHRP Recommended Provisions* update process.

2.6.3 Rapid Response: ShakeMaps

An important point in summarizing the present status of assessment of seismic strong ground motions is that in a number of countries, digital
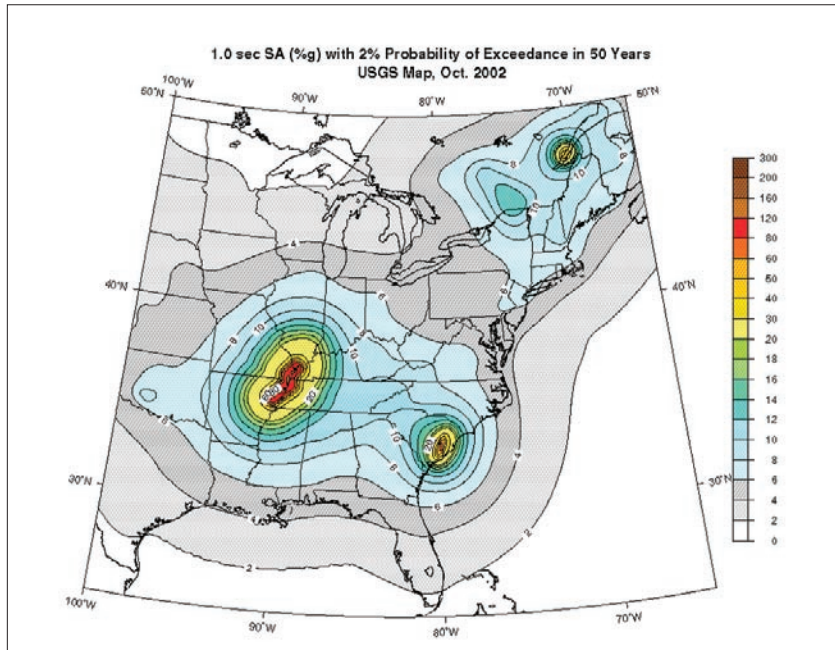
NATURE OF EARTHQUAKES AND SEISMIC HAZARDS

Figure 2-15: 1.0 second (long) period spectral acceleration values in %g with a 2% probability of exceedance in 50 years for central and southern United States.

SOURCE: USGS NATIONAL SEISMIC HAZARD MAPPING PROJECT.

strong-motion systems linked to communication centers (telephone, wireless, or satellite) have now been installed. These provide processed observational data within a few minutes after shaking occurs. The USGS **ShakeMap** program produces a computer-generated representation of ground shaking produced by an earthquake. (Figure 2-16) The computation produces a range of ground shaking levels at sites throughout the region using attenuation relations that depend on distance from the earthquake source, and the rock and soil conditions through the region so that the observed strong ground motions can be interpolated. One format of the maps contours peak ground velocity and spectral acceleration at 0.3, 1.0, and 3.0 seconds and displays the locational variability of these ground motion parameters.

Not only peak ground acceleration and velocity maps are computed using instrumental measurements, but by empirical correlations of the various scales, approximate Modified Mercalli Intensity estimates are also
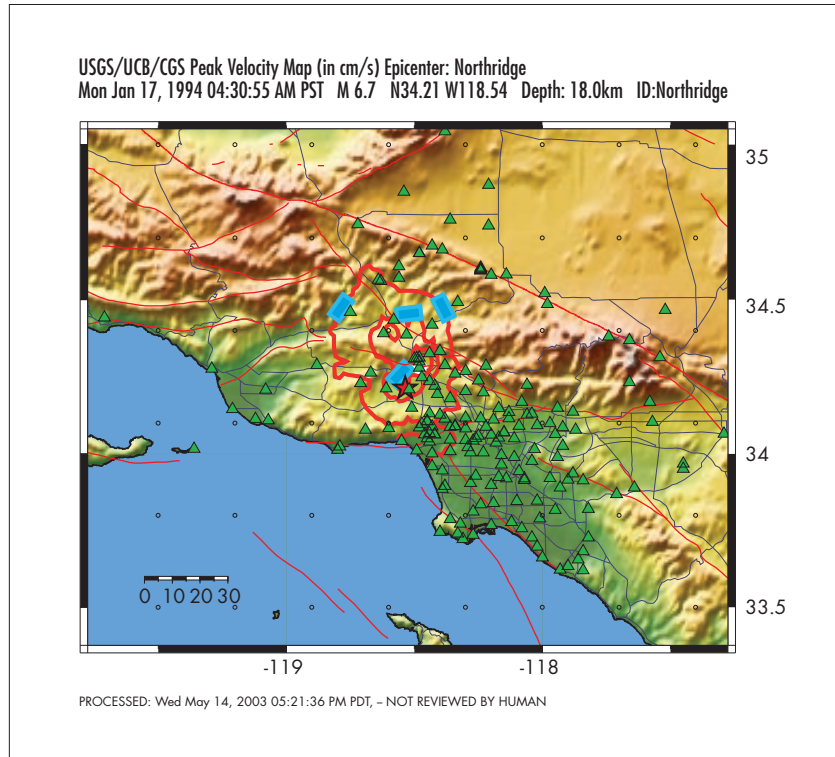
USGS/UCB/CGS Peak Velocity Map (in cm/s) Epicenter: Northridge
Mon Jan 17, 1994 04:30:55 AM PST   M 6.7   N34.21 W118.54   Depth: 18.0km   ID:Northridge

PROCESSED: Wed May 14, 2003 05:21:36 PM PDT, – NOT REVIEWED BY HUMAN

Figure 2-16: Example of a peak ground velocity (PGV) ShakeMap for the 1994 M_w=6.7 Northridge earthquake.

Strong-motion stations are shown as triangles, the epicenter as a red star, and thick red lines show contours (30, 60, and 90 cm/s) of PGV. Directivity during the rupture process causes the largest amplitudes to be located significantly to the north of the epicenter.

mapped. These maps make it easier to relate the recorded ground motions to the felt shaking and damage distribution. In a scheme used in the Los Angeles basin, the Instrumental Intensity map is based on a combined regression of recorded peak acceleration and velocity amplitudes (see Wald et al., 1999).

In 2001, such ShakeMaps for rapid-response purposes became available publicly on the Internet (see Section 2.10) for significant earthquakes in the Los Angeles region and the San Francisco Bay Area of California. Similar maps are available in other countries. Additionally, efforts are underway to combine near-real-time knowledge about the earthquake source process with the observed strong ground motions to produce maps that may better take into account the effects due to directivity.

NATURE OF EARTHQUAKES AND SEISMIC HAZARDS

ShakeMaps represent a major advance not only for emergency response, but also for scientific and engineering purposes. Their evolution and improvement will no doubt be rapid.

2.7 CONCLUSIONS

The seismological methods dealt with in this chapter will no doubt be much extended in subsequent years. First, greater sampling of strong-ground motions at all distances from fault sources of various mechanisms and magnitudes will inevitably become available. An excellent example of seismic recording growth comes from the 1999 Chi-Chi, Taiwan, earthquake.

Another interesting recent case is the major Alaska earthquake of November 3, 2002. This 7.9 magnitude earthquake was caused by rupture along the Denali fault for 200 km, with right-lateral offsets up to 10 m. A number of strong-motion records were obtained; the Trans-Alaskan oil pipeline did not suffer damage because of an innovative pipeline design combined with sophisticated knowledge of the seismology.

Second, more realistic 3D numerical models will solve the problem of the sequential development of the wave mixtures as the waves pass through different geological structures. Two difficulties may persist: the lack of knowledge of the roughness distribution along the rebounding fault and, in many places, the lack of quantitative knowledge of the soil, alluvium, and crustal rock variations in the region. For these reasons, probabilistic estimation as a basis of engineering decisions seems preferable.

Over the past decade, advances in digital seismometry have greatly reduced the recovery and computer processing time of recorded data, producing near-real time analysis products important for post-earthquake emergency response (Gee et al., 1996; Dreger and Kaverina, 2000; Wald et al., 1999). Continuing improvements in technology are expected to further increase the amount of timely earthquake source and strong ground motion information. A recent significant advance in general motion measurement is correlation with precisely mapped co-seismic ground deformations, and efforts are currently underway to obtain and analyze these data in near-realtime. Networks of continuous, high-

sample-rate **Global-Positioning-System** (GPS) instruments will no doubt help greatly in future understanding of the source problem and the correct adjustment to strong-motion displacement records.

A broad collection of standardized strong-motion time histories is now being accumulated in virtual libraries for easy access on the Internet. Such records will provide greater confidence in seismologically sound selection of ground motion estimates.

Additional instrumentation to record strong ground motion remains a crucial need in earthquake countries around the world. Such basic systems should measure not only free-field surface motions, but also downhole motions to record the wave changes as they emerge at the earth's surface.

The Advanced National Seismic System (ANSS) program is a major USGS and NEHRP initiative that provides accurate and timely information on seismic events. It is working to unify seismic monitoring in the United States, and provides a framework to modernize instrumentation and revolutionize data availability for research, engineering and public safety. (For more information, see http:www.anss.org/.)

In particular, many contemporary attenuation estimates for ground velocity and displacement will no doubt be improved as more recorded measurements are included, rendering earlier models obsolete. The statistical basis for separation of the probability distributions as functions of the various key parameters will become more robust. To keep abreast of changes, ground motion attenuation model information may be found at the USGS Earthquake Hazards Program website (see Section 2.10).

2.8 ACKNOWLEDGMENTS

2.9 CITED AND OTHER RECOMMENDED REFERENCES

Abrahamson, N. A. and W. Silva, 1997, Empirical response spectral attenuation relations for shallow crustal earthquakes, *Seism. Res. Letters*, 68, 94-127.

Atkinson, G. M., and D. M. Boore, 1995, New ground motion relations for eastern North America, *Bull. Seism. Soc.* Am., 85, 17-30.

Bolt, B. A., 1975, The San Fernando earthquake, 1971. *Magnitudes, aftershocks, and fault dynamics*, Chap. 21, Bull. 196, Calif. Div. of Mines and Geol., Sacramento, Calif.

Bolt, B. A. 2003. Engineering seismology, In: *Earthquake Engineering, Recent Advances and Applications*, eds. Y. Bozorgnia and V. V. Bertero, CRC press. Florida.

Bolt, B. A., 2003, *Earthquakes*, 5th edition, W. H. Freeman: New York.

Comerio, M., 1998. *Disaster Hits Home*, University of California Press: Berkeley.

FEMA 450, NEHRP (National Earthquake Hazards Reduction Program) *Recommended Provisions and Commentary for Seismic Regulations for New Buildings and Other Structures*, 2003 Edition, Federal Emergency Management Agency, Washington, DC

Gee, L. S., D. S. Neuhauser, D. S. Dreger, M. Pasyanos, R. A. Uhrhammer, and B. Romanowicz, 1996, Real-time seismology at UC Berkeley: The Rapid Earthquake Data Integration Project, *Bull. Seism. Soc. Am.*, 86, 936-945.

Hanks, T C, and H. Kanamori, 1979. A moment magnitude scale, *Journ. Geophys. Res.*, 84, 2348-2350.

International Code Council, *International Building Code* (IBC), 2003, Falls Church, VA

National Fire Protection Association, NFPA 5000, *Building Construction and Safety Code* , 2006, , Quincy,MA

Olsen, K.B., R.J. Archuleta, and J.R. Matarese (1995). Three-dimensional simulation of a magnitude 7.75 earthquake on the San Andreas fault, *Science*, 270, 1628-1632.

Stein, R. S., 2003, Earthquake Conversations, *Scientific American*, Vol. 288, No. 1, 72-79.

Yeats, R. S., C. R. Allan, K. E. Sieh, 1997. *The Geology of earthquakes*, Oxford University Press.

Yeats, R. S., 2001. *Living with Earthquakes in California: A Survivor's Guide*, Oregon State University Press: Corvallis.

2.10 WEB RESOURCES

Consortium of Organizations for Strong-Motion Observational Systems
COSMOS http://www.cosmos-eq.org

European Strong-Motion Database (ISESD)
http://www.isesd.cv.ic.ac.uk/

National Seismic Hazard Mapping Project, Golden, Colorado
http://geohazards.cr.usgs.gov/eq/

ShakeMaps www.trinet.org/shake

Tsunami Warning Centers http://www.prh.noaa.gov/pr/ptwc/
http://wcatwc.gov/

USGS Earthquake Hazards Program http://earthquake.usgs.gov/